[Frontiers in Bioscience 13, 3857-3868, May 1, 2008]

4-Thiazolidinones: a novel class of hepatitis C virus NS5B polymerase inhibitors

Neerja Kaushik-Basu[1], Alain Bopda-Waffo[1], Tanaji T. Talele[2], Amartya Basu[1], Ye Chen[1], S. Guniz Kucukguzel[3]

[1]Department of Biochemistry and Molecular Biology, UMDNJ-New Jersey Medical School, 185 South Orange Avenue, Newark, NJ 07103, [2]Department of Pharmaceutical Sciences, College of Pharmacy and Allied Health Professions, St. John's University, Jamaica, NY 11439, [3]Marmara University, Faculty of Pharmacy, Department of Pharmaceutical Chemistry, Haydarpasa, 34668 Istanbul, Turkey

TABLE OF CONTENTS

1. ABSTRACT

In a quest to identify novel compounds targeting HCV viral replicase, we evaluated a new series of 4-thiazolidinone derivatives (18 compounds). Our *in vitro* NS5B RdRp inhibition analysis with a series of 2′,4′-difluoro-4-hydroxybiphenyl-3-carboxylic acid [2-(5-nitro-2-furyl / substituted phenyl)-4-thiazolidinone-3-yl] amides (**1-7**) yielded IC_{50} values ranging between 45-75 microM. Of these, lead compound **6**: 2′,4′-difluoro-4-hydroxybiphenyl-3-carboxylic acid[2-(2-fluorophenyl)-4-thiazolidinone-3-yl]amide exhibited an IC_{50} value of 48 microM and inhibited NS5B non-competitively with respect to UTP and exhibited a mixed mode of inhibition with respect to RNA. Molecular docking of thiazolidinone derivatives within the allosteric site of NS5B yielded significant correlation between their calculated binding affinity and IC_{50} values. Taken together, these data suggest that the 4-thiazolidinone scaffold may be optimized for generating new analogues with improved anti-NS5B potency.

2. INTRODUCTION

Hepatitis C virus (HCV), identified in 1989 as the etiological agent of parenteral non-A non-B hepatitis, often causes the development of malignant chronic disease including liver cirrhosis and hepatocellular carcinoma frequently resulting in death (1-3). With an estimated 3% of the global population infected with HCV, including 4.1 million in the United States alone, and no protective vaccine available at present, this disease has emerged as a serious global health problem (4,5). Although significant advances have been made in the development of treatments for chronic hepatitis C, their efficacy is not universal and only 50% success has been reported in achieving a sustained viral response for the current combination therapy with new pegylated (PEG) forms of interferon plus ribavirin (6-9). Moreover, this therapy has considerable liabilities including significant adverse side effects and high cost, thus highlighting the need to develop improved therapeutic options to combat HCV infections (10).

HCV is an enveloped, positive-stranded RNA virus. Its single-stranded ~9.6 kb RNA genome encodes a large polyprotein of ~3010 amino acids comprising 4 structural proteins (Core, E1, E2, and p7) and 6 nonstructural proteins (NS2, -3, -4A, -4B, -5A, and -5B) (11-13). One of the NS proteins, NS5B, an RNA-dependent RNA polymerase (RdRp) is the most studied target for anti-HCV therapy as it is crucial and unique component of the viral replication machinery (7,9,14-19). NS5B, a 68 kDa membrane-associated protein contains motifs shared by all RdRps in which the catalytic domain is arranged around a central cleft in an organization that resembles a right hand, with the "palm" "finger" and "thumb" subdomains common to polymerases (20,21). Recombinant expression of active, soluble NS5B in a variety of systems has been achieved by various C-terminal deletions between 21 and 55 amino acid residues and its biochemical properties investigated (22-31). All of these reported recombinant HCV RdRps utilize a wide range of RNAs as template *in vitro* without preference, although they do prefer certain homo-polyribonucleotides to others and their activity is stimulated by GTP under specified conditions (29,31-34). Many screening assays for NS5B inhibitors utilize synthetic homopolymeric templates/primers (35-39). NS5B inhibitors thus far identified by these screening procedures can be broadly classified as either nucleoside (NI) or non-nucleoside (NNI) inhibitors (14,40).

The 4-thiazolidinone class of NNIs constitutes a promising category of compounds with versatile biological activity profile. These include antimycobacterial, antibacterial, and antifungal activities (40-42). The antiproliferative property of these compounds has also been explored to develop them as anti–tumor and anti-inflammatory agents specifically targeting the cyclooxygenase (COX) enzymes (43,44). Numerous studies have elucidated the potent antiviral properties of thiazolidinones against HIV-1 and in recent years these compounds have been extensively pursued as HIV-1 RT inhibitors (45-47).

In this study, we have explored the therapeutic potential of the thiazolidinone scaffold against HCV NS5B employing a panel of 4-thiazolidinone derivatives which were previously synthesized by Kucukguzel *et al.* (42,48). The inhibitory potency of 4-thiazolidinone ring system against HCV replicase has not been examined to-date. Our investigations have focussed on building the structure–activity relationship (SAR) around 2- and 3-positions of the 4-thiazolidinone template in contrast to the recently reported 4-oxo-2-thionothiazolidines which carry arylsulfonamido and arylidene substituents at 3- and 5-positions, respectively (49). Here we report the potency and mode of action of these compounds against HCV NS5B RdRp. These investigations should aid in the development of novel 4-thiazolidinone compounds harboring potent anti-NS5B activity.

3. MATERIALS AND METHODS

3.1. Synthesis of inhibitors

The 2′,4′-difluoro-4-hydroxybiphenyl-3-carboxylic acid[2-(5-nitro-2-furyl / substituted phenyl)-4-thiazolidinone-3-yl]amides (**1-7**); 2-(2′,4′-difluoro-4-hydroxybiphenyl-3-carbonyl-hydrazono)-3-alkyl / aryl-4-thiazolidinones (**8-10**); 2-[4-(4-methoxy-benzoylamino)benzoylhydrazono]-3-alkyl-4-thiazolidinones (**11-13**) and 2-substituted-3-{[4-(4-methoxybenzoylamino)benzoyl]amino}-4-thiazolidinones utilized in this study (Table 1) were synthesized as described previously (42,48). The purity of the compounds was greater than 95% as assessed by ^{1}H NMR and ^{13}C NMR spectroscopy. The compounds were dissolved in 100% dimethylsulphoxide (DMSO) as a 30-50 mM stock solution and stored at -20^{o}C for no more than 2 weeks. Serial dilutions were made in DMSO just prior to the assay.

3.2. Purification of recombinant replicase proteins

Plasmid pThNS5BCdelta21 was transformed in *Escherichia coli* DH5alpha and used for purification of HCV NS5BCdelta21 as previously described (30,50). The plasmid pet24b-SARS-CoV-nsp12 was transformed in *E. coli* BL21 STAR DE3 (Invitrogen) to express a C-terminally His-tagged SARS-CoV RdRp. The cells were cultured in LB medium supplemented with kanamycin (30 microgram/mL) at 37°C until the culture density (A_{600}) reached 0.6. After induction of expression with 0.2 mM isopropyl-beta-D-1-thiogalactopyranoside (IPTG), the cells were grown for 16 h at 18°C. Cells were harvested and the His-tagged nsp12 was purified by Ni-NTA affinity chromatography as described for HCV NS5B. Identity of the purified SARS-CoV-nsp12-His protein was confirmed by western blotting employing the His-probe (H3, Santa Cruz Biotechnology) mouse monoclonal primary antibody and goat anti-mouse horseradish peroxidase conjugated secondary antibody (Rockland Immunochemicals). Membrane-bound antibodies were detected with the ECL enhanced chemiluminescence kit (Santa Cruz Biotechnology).

3.3. RNA-dependent RNA polymerase (RdRp) assay

The RdRp activity of NS5B was evaluated by the standard primer-dependent elongation reactions employing poly rA/U_{12} template-primers (TP). Reaction mixtures containing 20 mM Tris-HCl (pH 7.0), 100 mM NaCl, 100 mM Na-glutamate, 0.5 mM DTT, 0.01% BSA, 0.01% Tween-20, 5% glycerol, 20 U/ml of RNasin, 0.5 microM of poly rA/U_{12}, 25 microM UTP, 2-5 microCi [alpha-^{32}P]UTP, 500 ng of NS5BCdelta21 and 0.5 mM $MnCl_2$ with or without inhibitors in a total volume of 25 microliters were incubated for 1 h at 30°C. Reactions were quenched by the addition of ice cold 5% (v/v) trichloroacetic acid (TCA) containing 0.5 mM pyrophosphate (PPi), the denatured polymeric RNA products were transferred to GF-B filters and the amount of radioactive UMP incorporated into RNA products was quantified on a liquid scintillation counter (Packard). The concentrations of the compounds inhibiting 50% of NS5B RdRp activity (IC_{50}) were calculated from the inhibition curves as a function of inhibitor concentration. Nsp12 activity was similarly evaluated except that incubations were carried out at 25°C for optimal enzymatic activity.

Incorporation of UMP on poly rA/U_{12} template-primer by NS5BCdelta21 at varying compound

Table 1. Structure-activity relationship of the 4-thiazolidinone derivatives

1-7

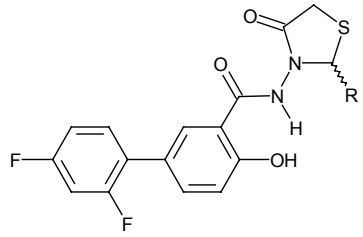

8-10

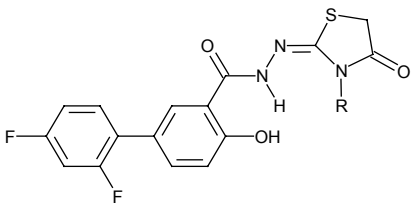

11-13

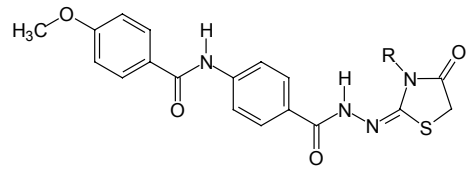

14-18

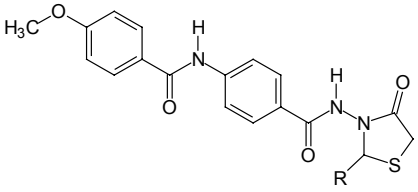

Compound	R	Binding Affinity	HCV NS5B		SARS nsp12
		Gscore (kcal/mol)[1]	%Activity	IC_{50}(microM)	%Activity
1	Phenyl	-6.08	20	73	56
2	4-fluorophenyl	-6.64	18	65	66
3	4-chlorophenyl	-0.69	42	over 100	78
4	4-methylphenyl	-4.45	16	63	88
5	5-nitro2-furyl	-5.01	25	78	NI[2]
6	2-fluorophenyl	-6.97	8	48	74
7	3-fluorophenyl	-4.34	23	77	88
8	Methyl	+0.27	55	-	73
9	Allyl	-0.94	48	-	42
10	Ethyl	+0.88	52	-	70
11	Methyl	-	61	-	49
12	Ethyl	-	76	-	47
13	Allyl	-	NI[2]	-	NI[2]
14	5-nitro2-furyl	-	60	-	NI[2]
15	4-fluorophenyl	-	58	-	NI[2]
16	4-chlorophenyl	-	78	-	88
17	4-bromophenyl	-	65	-	51
18	4-hydroxy-3-ethoxyphenyl	-	50	-	54

Percent activity was determined at 0.5 mM concentration of the indicated compound. NS5B RdRp activity in the absence of the inhibitor was taken as 100 percent after subtraction of residual background activity (Activity in the absence of the enzyme). IC_{50} values of the compounds 1-7 were determined from dose–response curves using 8-12 concentrations for each compound in duplicate. Curves were fitted to data points using nonlinear regression analysis and IC_{50} values were interpolated from the resulting curves using GraphPad Prism software. Values represent an average from at least three independent experiments. [1] A more negative Gscore indicates a better fit at the binding site. [2] NI = not inhibitory.

concentrations was visualized qualitatively by gel analysis of reaction products essentially as described above for the HCV RdRp assay except that the elongation time was reduced to 20 min. Reactions were stopped by the addition of 25 mM EDTA-0.5% SDS, subjected to phenol-chloroform extraction and ethanol precipitation and the recovered RNA products were dissolved in formamide gel loading buffer and resolved on a denaturing 12% polyacrylamide gel containing 7 M urea. The extent and pattern of synthesis was visualized by phosphorimaging (Molecular Dynamics).

The primer-independent de novo initiation activity of NS5B in the presence of compound 6 was reconstituted on HCV plus-strand 5′-UTR RNA template under conditions as previously described (38). Synthesis of the HCV plus-strand 5′-UTR run-off RNA transcript was carried out *in vitro* employing the HCV 5' UTR PCR product carrying the T7 RNA polymerase promoter at its 5' terminus as template and the T7 RNA polymerase kit (Roche) in accordance with the manufacturer's procedure.

Reactions involving the modified order of addition reaction required pre-incubation of the reaction components specified in figure-legend 3 and were carried out essentially as described by Lee *et al.* (49).

3.4. Cross-linking of NS5B to TP

A synthetic rA_{20}/U_{12} template-primer was employed for cross-linking of NS5B to RNA. The U_{12}-primer was 5′-end-labeled with [gamma-^{32}P] ATP using T4 polynucleotide kinase, purified on a NAP-10 column (GE Healthcare), adjusted to the required specific radioactivity with unlabeled primer and annealed with equimolar concentrations of unlabeled rA_{20} template. Cross-linking reactions as a function of inhibitor concentration were carried out as described earlier (51). Briefly, 50 microliters reaction mixture containing 20 mM Hepes (pH 7.0), 50

mM NaCl, 0.5 mM DTT, 0.01% BSA, 5% (v/v) glycerol, 20 U/ml of RNasin, 200 nM of ^{32}P-labeled U_{12}/rA_{20} (15,000 cpm/pmol), 1.5 micrograms of NS5BCdelta21 and 0.5 mM $MnCl_2$ was incubated on ice for 10 min in the absence or increasing concentrations of the inhibitor and exposed to 254 nm UV irradiation at a dose of 300 mJ/cm^2 (Spectronic Corp.). The cross-linked species were resolved by SDS-PAGE (8%). The dried gel was analyzed on a phosphorimager and the extent of cross-linking was quantified using ImageQuant software (Molecular Dynamics).

3.5. Determination of the *Ki* and mode of inhibition

The mode of inhibition by the most potent inhibitor was evaluated essentially in two series of experiments as described by McKercher *et al.*(38). The first series of experiments was performed by varying the template/primer (poly rA/U_{12}) and inhibitor concentrations. The concentration of poly rA/U_{12} ranged from 0.2 to 2.5 microM with a fixed concentration of UTP at 25 microM. In the second set of experiments, reaction velocities were determined at a fixed concentration of poly rA/U_{12} (0.25 microM) and varying concentrations of inhibitor and UTP (ranging from 2.5 to 80 microM). In both series of experiments, the concentration of inhibitor 6 ranged 1-3 times its IC_{50} value. Assays were carried out in the standard RdRp buffer containing 500 ng of NS5BCdelta21 and 3-6 microCi [alpha-^{32} P] UTP. Aliquots were withdrawn at defined times, terminated by quenching with 5% (v/v) TCA-0.5 mM PPi and the incorporation of radiolabel UMP into RNA product was determined by GF-B filter binding assay. Data was plotted according to the methods of Dixon and Cornish-Bowden (52) in order to determine the mode of inhibition and the constant(s) of inhibition (*Ki*). The experiments were performed at least twice and values represent an average of at least triplicate samples. Standard deviations for all *Ki* were less than 10%.

3.6. Molecular Modeling

All computations were carried out on a Dell Precision 470n workstation with the RHEL 4.0 operating system using Glide 4.5 (Schrodinger, LLC, New York). Using a recently solved HCV NS5B polymerase co-crystal structure with N-benzylphenylalanine inhibitor as a template, compounds **1-10** were docked into the allosteric binding site of NS5B (PDB ID: 1NHU) (53) using the extra precision (XP) Glide 4.5 docking program . For docking experiments all the compounds were constructed using the fragment dictionary of Maestro 8.0 and geometry optimized using the Optimized Potentials for Liquid Simulations-all atom (OPLS-AA) force field (54) with the steepest descent followed by truncated Newton conjugate gradient protocol as implemented in the Macromodel 9.5. Water molecules of crystallization were removed from the complex, and the protein was optimized for docking using the protein preparation wizard provided by Schrodinger LLC and the Impact program (FirstDiscovery v4.5). Partial atomic charges for compounds as well as protein were assigned according to the OPLS-AA force field. Although details on the methodology used by Glide are described elsewhere (55-58), a short description is provided below. The binding site, for which the various energy grids were calculated and stored, is defined in terms of two concentric cubes: the bounding box, which must contain the center of any acceptable ligand pose, and the enclosing box, which must contain all ligand atoms of an acceptable pose. Cubes with an edge length of 12 Å and centered at the midpoint of the longest atom-atom distance in the respective cocrystallized ligand defined the bounding box in the protein. Similarly, the larger enclosing box was defined in terms of the cocrystallized ligand with an edge length of 30 Å. Poses with a root mean square deviation (rmsd) of less than 0.5 Å and a maximum atomic displacement of less than 1.3 Å were eliminated as redundants to be able to increase diversity in the retained ligand poses. The scale factor for van der Waals radii was applied to those atoms with absolute partial charges less than or equal to 0.15 (scale factor of 0.8) and 0.25 (scale factor of 1.0) electrons for ligand and protein, respectively. The *maxkeep* variable which sets the maximum number of poses generated during the initial phase of the docking calculation were set to 5000 and the *keep best* variable which sets the number of poses per ligand that enters the energy minimization was set to 1000. Energy minimization protocol includes dielectric constant of 4.0 and 1000 steps of conjugate gradient. Upon completion of each docking calculation, 100 poses per ligand were allowed to generate. The top-scored pose was selected using a Glidescore (Gscore) function. The Gscore is a modified and extended version of the empirically based Chemscore function (59). The docking methodology was validated by extracting the crystallographic bound N-benzylphenylalanine inhibitor and redocking it to the allosteric binding site of NS5B. This validation provided a root mean square deviation (rmsd) of 0.748 angstrom between the docked versus the experimental conformation.

4. RESULTS

4.1. Expression and purification of recombinant replicase proteins

The effect of the 4-thiazolidinone derivatives on the RdRp activity of NS5B was evaluated on His-tagged HCV NS5B polymerase (genotype 1b), lacking the C-terminal 21-amino acid residues (NS5BCdelta21). Deletion of the last 21 hydrophobic residues of NS5B has been reported to enhance protein solubility (28), without compromising its kinetic properties or its ability to perform both *de novo* and primer-initiated RNA synthesis (60,61). Recombinant NS5BCdelta21 (64 kDa) purified on a Ni-NTA affinity chromatography column exhibited purity of more than 95% as visualized by Coomassie blue staining of the SDS-PAGE (Figure 1A, lane 1). On the other hand, purification of recombinant SARS nsp12 protein on a Ni-NTA affinity resin yielded two protein bands corresponding to 107 kDa and 74 kDa. Proteomic analysis of these two bands confirmed their identity as SARS nsp12 and *E. coli* formyl transferase, respectively (Figure 1A, lane 2). The identity of SARS nsp12 was also confirmed by imunoblotting employing anti-His antibody (Figure 1A, lane 3). The implication of this co-elution and functional analysis of SARS nsp12 will be discussed elsewhere (manuscript under preparation).

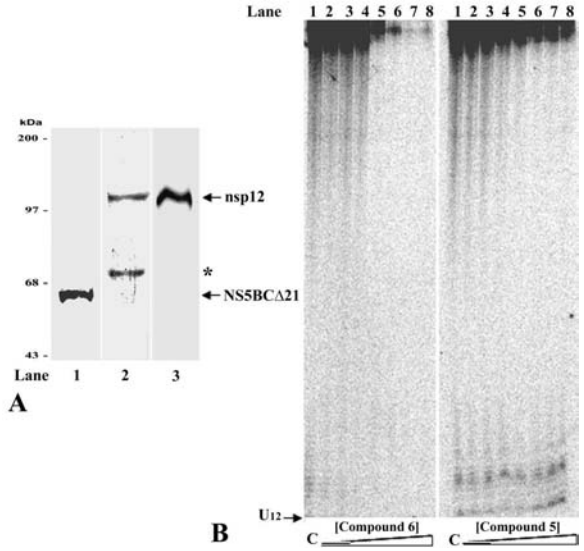

Figure 1. 4-Thiazolidinone derivatives inhibit HCV NS5B RdRp activity. (A) Purification of recombinant 6X His-tagged HCV NS5BCdelta21 (lane 1) and SARS-CoV nsp12 (lane 2) proteins from E. coli BL21 (DE3) using a Ni-NTA affinity column. The positions of the purified proteins are indicated by an arrow to the right of the gel. The molecular weight markers are shown on the left of the gel. The 74 kDa band in lane 2 indicated by an asterisk represents the co-purified protein *E. coli* formyl transferase. Purified nsp12 was confirmed by imunoblotting with anti-His antibody (lane 3). (B) Characterization of products of NS5B RdRp assay in a denaturing polyacrylamide gel in the presence and absence of indicated compound. Lane 1, NS5B activity in the absence of the inhibitors; lanes 2–8 represent indicated compound concentrations of 10, 25, 50, 100, 250, 500 and 1250 microM. The position of the U_{12}-primer is indicated by an arrow to the left of the gel.

4.2. Identification of 4-thiazolidinones as inhibitors of HCV NS5B RdRp activity

In a quest for inhibitors of HCV NS5B RdRp activity, we screened 18 compounds carrying the 4-thiazolidinones scaffold (Table 1). The compounds were first dissolved into DMSO, and then transferred into the assay buffer. To get an idea of the inhibitory potency of these compounds, preliminary screening was conducted at compound concentrations of 0.5 mM. As seen in Table 1, while compound **13** showed no inhibitory activity, the 17 other thiazolidinone derivatives exhibited a wide range of anti-NS5B potency (8-78% activity). The overall trend indicated a greater inhibition with compounds **1-7** in comparison to compounds **8-18**. We therefore evaluated the IC_{50} values for compounds 1-7 by monitoring the total incorporation of radiolabeled UTP on poly rA/U_{12} as a function of inhibitor concentration. Compounds 1-7 yielded an IC_{50} value ranging from 45-100 microM (Table 1). Of these, compound 6 exhibiting an IC_{50} value of 48 microM was found to be the most potent, in contrast to compound 3 (IC_{50} more than 100 microM), the least potent compound of this series. The other compounds exhibited near equipotent activity (63-78 microM).

We were curious to examine if the inhibition mediated by the thiazolidinone derivatives resulted in abortive synthesis of the RNA products. This prompted us to investigate the nature and pattern of the RNA product synthesized by NS5B as a function of inhibitor concentration by gel based analysis of the reaction products. Similar assays have been reported by several groups in context of NS5B-inhibition mechanism on a variety of template-primers (38,49,62-64). Figure 1B depicts a representative image of this analysis. Both compounds **5** and **6** inhibited full-length product formation in a concentration-dependent manner (Figure 1B, lanes 2 to 8). Consistent with their respective IC_{50} values, compound **6**, the most potent compound exhibited higher extent of inhibition compared to compound **5** at similar concentrations, with near absence of product synthesis at higher inhibitor concentrations (Figure 1B, lanes 6-8). The reactions containing inhibitors did not appear to produce shorter products as a result of abortive initiation or premature termination.

To determine the specificity of these compounds for HCV NS5B, we examined the inhibitory effect of the compounds against non-structural protein 12 (nsp12), the RNA-dependent RNA polymerase (RdRp) of severe acute respiratory syndrome virus (SARS-CoV) (65,66). Details pertaining to the purification and characterization of a functionally active SARS-CoV nsp12 protein of 932 amino acids will be described elsewhere (Figure 1A, manuscript in preparation). The RdRp activity of nsp12 in the absence or presence of the individual compounds (0.5 mM) was evaluated on poly rA/U_{12}. As seen in Table 1, the inhibition pattern with this panel of compounds differed substantially for these two RdRps. While, all compounds showed substantially reduced potency against nsp12, four of the 18 thiazolidinone derivatives displayed no inhibitory effect. Notably, compounds **1-7** found to be most potent against NS5B displayed substantially reduced efficacy against nsp12. According to a recent structural model, SARS-CoV RdRp lacks the equivalent hydrophobic non-nucleoside binding pocket of HIV-1 RT as well as the non-nucleoside inhibitor-binding pocket of HCV NS5B (67). Our data substantiates this model and suggests that non-nucleoside inhibitors of HIV-RT and HCV NS5B may not be effective against SARS-CoV RdRp.

4.3. Mechanism of inhibition

To better understand the mechanism by which these compounds inhibit the RdRp activity of NS5B, the most potent inhibitor (compound **6**) from this SAR study was selected for further characterization. Toward this objective, two different series of kinetic analyses were performed in which reaction velocities were measured over a range of concentrations of template/primer, NTP and compound **6**. The data obtained were analyzed by Dixon and Cornish-Bowden plots for kinetic parameters and mode of inhibition (52). Reciprocal plots of reaction velocity revealed that compound **6** displayed a mixed mode of inhibition towards the template/primer, with a significant competitive component (K_i competitive = 55.7 microM) and a minor uncompetitive component (K_i uncompetitive = 91.5 microM) as deduced from the location of the

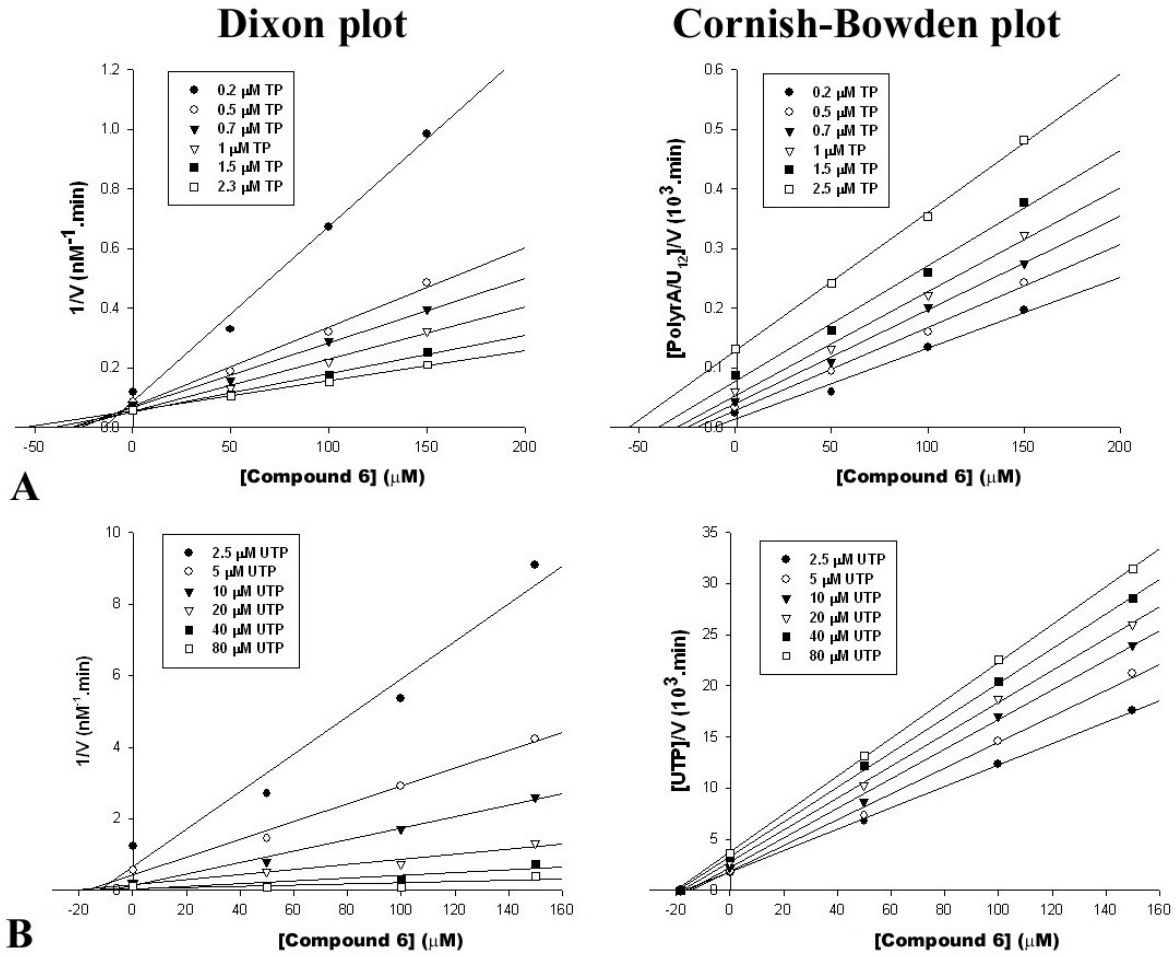

Figure 2. Evaluation of mode of inhibition and kinetic parameters of compound 6 with regard to template/primer and UTP substrates. Two sets of reactions were carried out. In one set, reaction velocities were measured at varying template/primer concentrations (0.2-2.3 microM) with the concentration of UTP fixed at 25 microM (Panel A). In another set, poly rA-U12 concentration was kept constant at 0.25 microM and reaction velocities were measured at increasing concentrations of UTP substrate (2.5–80 microM) in the absence or presence of increasing concentrations (50–150 microM) compound **6** (Panel B). Kinetic parameters were analyzed from the Dixon and Cornish-Bowden plots of the reciprocal velocity at indicated concentrations of compound **6**. Compound **6** exhibited a mixed mode of inhibition towards template/primer with a major competitive component (intercept on the Dixon plot above the x-axis) and a minor uncompetitive component (intercept extrapolated from the Cornish-Bowden plot below the x-axis) and corresponded to K_i competitive values of 55.7 microM and K_i uncompetitive values of 91.5 microM. In contrast, compound **6** displayed a non-competitive mode of inhibition with regard to UTP, reflected by an identical X-axis intercept on both the plots with K_i competitive= K_i uncompetitive=18.2 microM.

intercepts on the Dixon and Cornish-Bowden plots above and below the x-axis, respectively (Figure 2A). In contrast, the compound **6** demonstrated non-competitive inhibition with UTP substrate (K_i competitive = K_i uncompetitive = 18.2 microM), as all the lines converged reasonably well resulting in an X- intercept on both Dixon and Cornish-Bowden plots (Figure 2B). A similar mechanism of inhibition has also been demonstrated for another HCV NS5B non-nucleoside inhibitor belonging to the benzimidazole-5-carboxamide series (38).

To further clarify the mechanistic mode of inhibition by compound **6**, we examined its binding properties under varying conditions of pre-incubation with reaction components. Modification of the order of reagent addition, substantially affected the ability of compound **6** to inhibit the RdRp activity of NS5B, specifically under conditions of NS5B-RNA pre-incubation. As seen in Figure 3A, when compound **6** was pre-incubated with NS5B before the addition of template-primer, a modest drop in its IC_{50} value from 48 microM to 41.5 microM was observed (E+I). In addition, under these conditions a gradual near complete inhibition of NS5B activity was observed at compound **6** concentrations above 500 microM. This pattern of inhibition did not alter significantly when all three components were added together without pre-

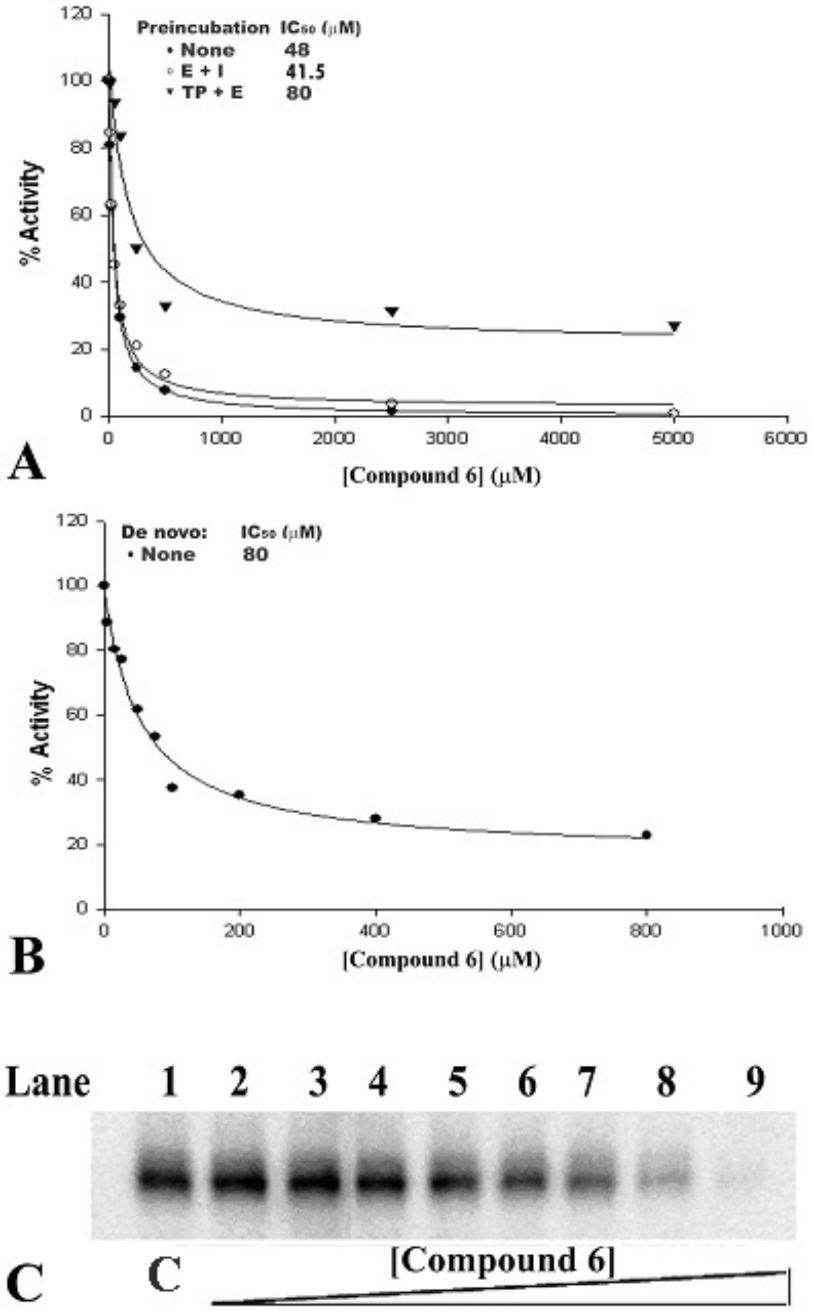

Figure 3. Effect of RNA on compound **6** Activity. (A) Dependence of inhibition curves on NS5B-RNA (TP+E) and NS5B-Inhibitor (E+I) complex formation was examined by pre-incubating the indicated components for 30 minutes at 4°C followed by evaluation of the NS5B RdRp activity. UMP incorporated into product was expressed as percent of control (no inhibitor) and plotted versus increasing concentrations of compound **6**. In another set, inhibition curves were obtained in the absence of pre-incubation of the reaction components (None). (B) Dose response curve displaying the IC_{50} of compound **6** in a NS5B de novo initiation assay employing HCV plus-strand 5′-UTR RNA template. The points on the curve represent an average of three independent determinations. (C) Effect of compound **6** on NS5B-RNA binary complex formation was evaluated by photochemical crosslinking. NS5B (1.5 microgram) was incubated with 30 nM [5′-^{32}P] labeled rA_{20}/U_{12} (200K Cerenkov cpm) in a binding buffer containing increasing concentrations of compound **6** and exposed to UV radiation. The cross-linked species were resolved by SDS-PAGE and the extent of NS5B-RNA cross-linking in the presence of the inhibitor was visualized by phosphorImaging and evaluated using Image-Quant software (Molecular Dynamics). Lane 1 in each set represents the control reaction carried out in the absence of the compound. Lanes 2–9 represent compound **6** concentrations of 5, 10, 25, 50, 100, 150, 200 and 400 microM, respectively.

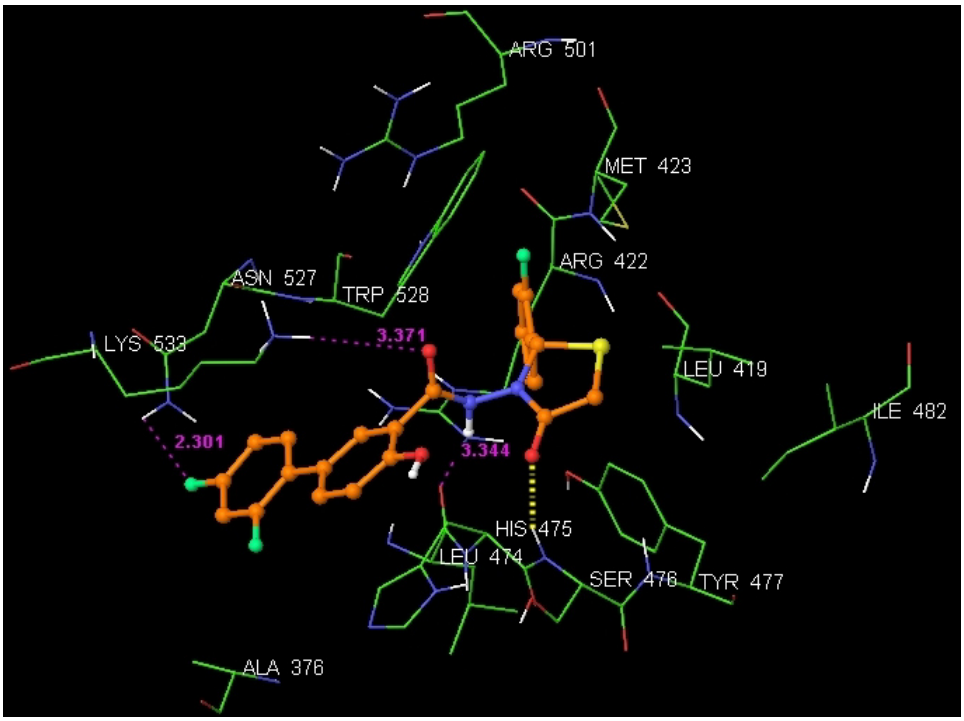

Figure 4. Docked model of the most potent compound **6** within the allosteric binding site of HCV NS5B polymerase. Hydrogen bonds are shown as dotted yellow lines while distances are shown as dotted pink lines. Active site amino acid residues are represented as sticks with the atoms according to the color scheme as carbon – green, nitrogen – blue, oxygen – red and sulfur – yellow while the inhibitor is shown as ball and stick model with the same color scheme as above except carbons are represented in orange.

incubation. In contrast, the inhibition curves dramatically changed under conditions of NS5B-RNA pre-incubation, prior to the addition of compound **6** (TP+E) and was reflected in an upward shift of the IC_{50} value from 48 to 80 microM. We observed that the activity of a substantial fraction of NS5B was not decreased even at very high concentrations of the inhibitor under condition of NS5B+RNA pre-incubation. This observation is consistent with the kinetic data and mode of inhibition suggesting that pre-incubation with RNA partially protected the enzyme from inhibition. A similar scenario has been reported for NNIs of NS5B polymerase based on benzimidazole and benzylidene scaffolds (38,49). Compound **6** also inhibited the primer-independent *de novo* initiation activity of NS5B on HCV plus-strand 5′-UTR RNA template (Figure 3B), though the efficacy was somewhat reduced (IC_{50} = 80 microM) when compared to primer elongation efficacy on homopolymeric RNA template (IC_{50} = 48 microM).

To understand if compound **6** mediated inhibition occurred at the step of NS5B-RNA binding, we cross-linked 5′-^{32}P-labeled rA_{20}/U_{12} to NS5B by UV irradiation in the presence of increasing amounts of the compound **6** and resolved the cross-linked species on a SDS-polyacrylamide gel as described earlier (51,68). As seen in Figure 3C (lanes 2 to 9), the NS5B–RNA complexed species decreased in direct proportion to inhibitor concentration, suggesting that inhibition may be mediated at the step of RNA binding step among others. This is in agreement with the competitive mode of TP binding and the protective effect displayed by RNA when pre-incubated with the enzyme.

4.4. Molecular Docking and Analysis of the Binding mode of compound 6

To investigate the differences in potency of the 4-thiazolidinone derivatives at a structural level and draw meaningful inferences from the SAR of these compounds, we performed docking studies. The binding affinity of the inhibitors is shown in Table 1. Compound **6** exhibited the high binding affinity in contrast to the lowest binding affinity obtained for the inactive compounds **3** and **8-10**. These values correlated well with the inhibitory potency of the compounds, thus validating the Glide molecular docking protocol.

We also analyzed the binding mode of compound **6** (Figure 4). Compound **6** was found to be engaged in a series of hydrogen bonding, hydrophobic, and van der Waals interactions with a shallow binding pocket which is close in space but clearly distinct from the binding site of GTP and the indole/benzimidazole-based ligands. The *ortho*-fluorophenyl moiety of the inhibitor was found to make hydrophobic contacts with Leu419, Met423, Trp528, and C_{beta}, C_{gamma}, C_{delta}, and $C_{epsilon}$ atoms of Arg422 and Arg501 residues. The 4-thiazolidinone moiety forms hydrophobic and van der Waals interactions with Leu419, Tyr477, and Ile482 residues. The carbonyl oxygen of the 4-thiazolidinone moiety was found to be engaged in hydrogen

Table 2. Structures and XPGlide-predicted Gscores of the newly designed analogues

New analogues 1-4			New analogues 5 and 6		
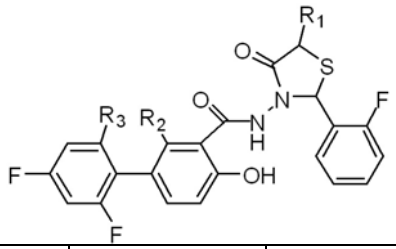			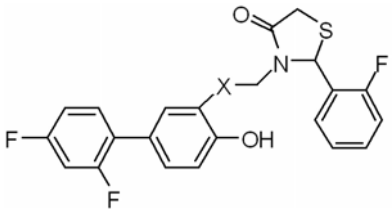		
New analogues	**R_1**	**R_2**	**R_3**	**X**	**Gscore kcal/mol**
1	-H	-H	-COOH	-	-8.48
2	-H	tetrazol-2-yl	-H	-	-7.50
3	-H	-H	tetrazol-2-yl	-	-7.24
4	$-CH_3$	-H	-H	-	-7.64
5	-	-	-	$-CH_2-$	-9.97
6	-	-	-	-C=O	-8.60

bonding interaction with the backbone atoms of Ser476 (O---HN, 2.10 angstrom, 155.0°). The –C=O and –NH groups of the hydrazide function were located at the hydrogen bonding distances from the side chain of Lys533 and the backbone of the Leu474, respectively. The biphenyl moiety is hosted in a pocket formed by the Ala376, Asn527, Lys533, and His475 residues. One of the phenyl rings of the biphenyl moiety was positioned to form pi-pi stacking interaction with His475. The *para*-fluoro substituent of the biphenyl moiety is engaged in strong electrostatic interaction with the side chain of Asn527. Interestingly, a recent study by Louise-May *et al.* has reported a spatially related similar binding mode by 5,4-dialkyl substituted thiophene analogues (69), thus supporting structure-based approach as a powerful tool to obtain novel lead compounds.

5. DISCUSSION

The binding mode of inhibitor **6** suggests ways to improve upon potency of thiazolidinone derivatives. Crystallographic data on NS5B-N-benzylphenylalanine complex suggest that Met423 side chain is very flexible and should accommodate bulkier groups (larger than *ortho*-fluorophenyl moiety) at the 2-position of the thiazolidinone moiety. Increasing the conformational flexibility of the thiazolidinone inhibitors may lead to potent analogues through cooperative binding within the allosteric site of NS5B. The conformational flexibility of the most potent inhibitor **6** can be achieved by bioisosteric replacement of the rigid amide function with freely rotatable functions such as an ethylene ($-CH_2-CH_2-$) or ketomethylene ($-COCH_2$) bridge between the biphenyl and thiazolidinone rings. The C-2 and C-5 positions of the thiazolidinone moiety establishes suboptimal hydrophobic interaction with the Leu419, Tyr477, and Leu482 residues, hence, a possibility of extending these positions by hydrophobic substituents would generate high binding affinity analogues through additional hydrophobic contacts. Further, a –COOH or a tetrazole group on the biphenyl moiety could potentially increase the affinity through ionic interaction of these groups with the side chain guanidine group of Arg422 and epsilon-NH_2 of the Lys533. Based on this structural insight, we hypothetically designed modified analogues of the most potent inhibitor (compound 6) and docked into the allosteric site of HCV NS5B polymerase. As seen in Table 2, the Gscores of these modified analogues were significantly improved over compound **6**, suggesting that these analogues may presumably be better inhibitors than compound **6**. This aspect is awaiting experimental verification pending synthesis of these analogues.

In conclusion, from the systematic SAR screening of the 4-thiazolidinone scaffold-based compounds employing HCV NS5B RdRp enzymatic assays, we identified a lead compound **6** which inhibited NS5B non-competitively with respect to UTP and exhibited a mixed mode of inhibition with RNA. Although the compound was not very potent (IC_{50} = 48 microM), characterization of its binding mode by biochemical and computational experiments suggest that the 4-thiazolidinone scaffold may be optimized for generating new analogues with improved anti-NS5B potency. Based on these studies, we are now in the process of synthesizing modified analogues of lead compound **6** in our laboratory for evaluating their effectiveness as potent NS5B RdRp inhibitors.

6. ACKNOWLEDGEMENTS

This research was supported by National Institute of Health (NIH) research grant R01-DK066837 and R21-AI059269 to NKB. TT was supported by start-up funds and resources provided by the College of Pharmacy and the Department of Pharmaceutical Sciences at St. John's University and SGK received research support from the Scientific Research Project Commission of Marmara University (Project number: HEA-DYD-052 / 051201, SAĞ-YY-010 / 020103 and 1998 / 62.).

.

7. REFERENCES

1. Q. L. Choo, G. Kuo, A. J. Weiner, L.R. Overby, D. W. Bradley, & M. Houghton: Isolation of a cDNA clone

derived from a blood-borne non-A, non-B viral hepatitis genome. *Science* 244, 359-62 (1989)
2. M. J. Alter, H. S. Margolis,K.Krawczynski, F.N. Judson, A. Mares, W.J. Alexander, P.Y. Hu, J.K. Miller, M. A. Gerber, R.E. Sampliner, & *et al.*: The natural history of community-acquired hepatitis C in the United States. The Sentinel Counties Chronic non-A, non-B Hepatitis Study Team. *N Engl J Med* 327, 1899-905 (1992)
3. P. Leyssen,E. De Clercq, & J. Neyts: Perspectives for the treatment of infections with Flaviviridae. *Clin Microbiol Rev* 13, 67-82 (2000)
4. A. Wasley, & M. J. Alter: Epidemiology of hepatitis C: geographic differences and temporal trends. *Semin Liver Dis* 20, 1-16 (2000)
5. M. J. Alter, D. Kruszon-Moran, O. V. Nainan, G. M. McQuillan, F. Gao, L. A. Moyer, , R. A. Kaslow, & H. S. Margolis: The prevalence of hepatitis C virus infection in the United States, 1988 through 1994. N Engl J Med 341, 556-62 (1999)
6. T. Hugle, & A. Cerny: Current therapy and new molecular approaches to antiviral treatment and prevention of hepatitis C. Rev Med Virol 13, 361-71 (2003)
7. J. F. Dillon: Hepatitis C: What is the best treatment? J Viral Hepat 11 Suppl 1, 23-7 (2004)
8. M. P. Walker, T. C. Appleby, W. Zhong, J. Y. Lau, & Z. Hong, Z. Hepatitis C virus therapies: current treatments, targets and future perspectives. Antivir Chem Chemother 14, 1-21 (2003)
9. Q. M. Wang, & B. A. Heinz: Recent advances in prevention and treatment of hepatitis C virus infections. Prog Drug Res 55, 1-32 (2000)
10. M. Cornberg, D. Huppe, J. Wiegand, G. Felten, H. Wedemeyer, & M. P. Manns: Treatment of chronic hepatitis C with PEG-interferon alpha-2b and ribavirin: 24 weeks of therapy are sufficient for HCV genotype 2 and 3. Z Gastroenterol 41, 517-22 (2003)
11. M. Hijikata, N. Kato,Y. Ootsuyama, M. Nakagawa, & K. Shimotohno: Gene mapping of the putative structural region of the hepatitis C virus genome by in vitro processing analysis. Proc Natl Acad Sci U S A 88, 5547-51 (1991)
12. A. Grakoui, C. Wychowski, C. Lin, S. M. Feinstone, & C. M. Rice: Expression and identification of hepatitis C virus polyprotein cleavage products. J Virol 67, 1385-95 (1993)
13. V. Lohmann, J. O. Koch, & R. Bartenschlager: Processing pathways of the hepatitis C virus proteins. J Hepatol 24, 11-9 (1996)
14. R. De Francesco, & C. M. Rice: New therapies on the horizon for hepatitis C: are we close? Clin Liver Dis 7, 211-42 (2003)
15. D. C. Myles: Recent advances in the discovery of small molecule therapies for HCV. Curr Opin Drug Discov Devel 4, 411-6 (2001)
16. A. M. Di Bisceglie, J. McHutchison, & C. M. Rice: New therapeutic strategies for hepatitis C. Hepatology 35, 224-31 (2002)
17. Z. L. Ni, & A. S. Wagman: Progress and development of small molecule HCV antivirals. Curr Opin Drug Discov Devel 7, 446-59 (2004)
18.Behrens, S. E., Tomei, L. & R. De Francesco: Identification and properties of the RNA-dependent RNA polymerase of hepatitis C virus. *Embo J* 15, 12-22 (1996)
19. C. H. Hagedorn, E. H. van Beers, & C. De Staercke Hepatitis C virus RNA-dependent RNA polymerase (NS5B polymerase). *Curr Top Microbiol Immunol* 242, 225-60 (2000)
20. S. Bressanelli, L. Tomei, F. A. Rey, & R. De Francesco: Structural analysis of the hepatitis C virus RNA polymerase in complex with ribonucleotides. *J Virol* 76, 3482-92 (2002)
21. R. A. Love, H. E. Parge, X. Yu, M. J. Hickey, W. Diehl, J. Gao H. Wriggers, A. Ekker, L. Wang, J. A. Thomson, P. S. Dragovich, & S. A. Fuhrman: Crystallographic identification of a noncompetitive inhibitor binding site on the hepatitis C virus NS5B RNA polymerase enzyme. *J Virol* 77, 7575-81 (2003)
22. T. Yamashita, S. Kaneko, Y. Shirota, W. Qin, T. Nomura, K. Kobayashi, & S. Murakami: RNA-dependent RNA polymerase activity of the soluble recombinant hepatitis C virus NS5B protein truncated at the C-terminal region. *J Biol Chem* 273, 15479-86 (1998)
23. R. De Francesco, S. E. Behrens, L. Tomei, S. Altamura, & J. Jiricny, J. RNA-dependent RNA polymerase of hepatitis C virus. *Methods Enzymol* 275, 58-67 (1996)
24. V. Lohmann, F. Korner, U. Herian, & R. Bartenschlager: Biochemical properties of hepatitis C virus NS5B RNA-dependent RNA polymerase and identification of amino acid sequence motifs essential for enzymatic activity. *J Virol* 71, 8416-28 (1997)
25. V. Lohmann, A. Roos, F. Korner,J. O. Koch, & R. Bartenschlager: Biochemical and kinetic analyses of NS5B RNA-dependent RNA polymerase of the hepatitis C virus. *Virology* 249, 108-18 (1998)
26. Z. H. Yuan, U. Kumar, H.C. Thomas, Y. M. Wen, & J. Monjardino: Expression, purification, and partial characterization of HCV RNA polymerase. *Biochem Biophys Res Commun* 232, 231-5 (1997)
27. R. H. Al, Y. Xie, Y. Wang, & C. H. Hagedorn: Expression of recombinant hepatitis C virus non-structural protein 5B in Escherichia coli. *Virus Res* 53, 141-9 (1998)
28. E. Ferrari, J. Wright-Minogue, J. W. Fang, B. M. Baroudy, J. Y. Lau, & Z. Hong Characterization of soluble hepatitis C virus RNA-dependent RNA polymerase expressed in Escherichia coli. *J Virol* 73, 1649-54 (1999)
29. K. Ishii, Y. Tanaka, C. C. Yap, H. Aizaki, Y. Matsuura, & T. Miyamura: Expression of hepatitis C virus NS5B protein: characterization of its RNA polymerase activity and RNA binding. *Hepatology* 29, 1227-35 (1999)
30. J. W. Oh, T. Ito, & M .M. Lai, M. M. A recombinant hepatitis C virus RNA-dependent RNA polymerase capable of copying the full-length viral RNA. *J Virol* 73, 7694-702 (1999)
31. L. Tomei, R. L. Vitale, I. Incitti, S. Serafini, S. Altamura, A. Vitelli, & R. De Francesco: Biochemical characterization of a hepatitis C virus RNA-dependent RNA polymerase mutant lacking the C-terminal hydrophobic sequence. *J Gen Virol* 81, 759-67 (2000)
32. V. Lohmann, H. Overton & R. Bartenschlager Selective stimulation of hepatitis C virus and pestivirus

NS5B RNA polymerase activity by GTP. *J Biol Chem* 274, 10807-15 (1999)
33. W. Zhong, A. S. Uss, E. Ferrari, J. Y. Lau, & Z. Hong: De novo initiation of RNA synthesis by hepatitis C virus nonstructural protein 5B polymerase. *J Virol* 74, 2017-22 (2000)
34. R. B. Johnson, X. L. Sun, M.A. Hockman, E. C. Villarreal, M. Wakulchik, & Q. M. Wang: Specificity and mechanism analysis of hepatitis C virus RNA-dependent RNA polymerase. *Arch Biochem Biophys* 377, 129-34 (2000)
35. T. J. Reddy, L.Chan, N. Turcotte, M. Proulx, O.Z. Pereira, S.K. Das, A. Siddiqui, W. Wang, C. Poisson, C.G. Yannopoulos, D. Bilimoria, L. L'Heureux, H. M. Alaoui, H. M. & N. Nguyen-Ba, Further SAR studies on novel small molecule inhibitors of the hepatitis C (HCV) NS5B polymerase. *Bioorg Med Chem Lett* 13, 3341-4 (2003)
36. L. Tomei, S. Altamura, L. Bartholomew, A. Biroccio, A. Ceccacci, L. Pacini, F. Narjes, N. Gennari, M. Bisbocci, I., Incitti, L. Orsatti, S. Harper, I. Stansfield, M.Rowley, R. De Francesco, & G. Migliaccio:. Mechanism of action and antiviral activity of benzimidazole-based allosteric inhibitors of the hepatitis C virus RNA-dependent RNA polymerase. *J Virol* 77, 13225-31 (2003)
37. P. L. Beaulieu, Y. Bousquet, J. Gauthier, J. Gillard, M. Marquis, G. McKercher, C. Pellerin, S. Valois, & G. Kukolj: Non-nucleoside benzimidazole-based allosteric inhibitors of the hepatitis C virus NS5B polymerase: inhibition of subgenomic hepatitis C virus RNA replicons in Huh-7 cells. *J Med Chem* 47, 6884-92 (2004)
38. G. McKercher, P.L. Beaulieu, D. Lamarre, S. LaPlante, S. Lefebvre, C. Pellerin, L. Thauvette, & G. Kukolj: Specific inhibitors of HCV polymerase identified using an NS5B with lower affinity for template/primer substrate. *Nucleic Acids Res* 32, 422-31 (2004)
39. G. Kukolj, G. A. McGibbon, G. McKercher, M. Marquis, S. Lefebvre, L. Thauvette, J. Gauthier, S. Goulet, M. A. Poupart, & P. L. Beaulieu: Binding site characterization and resistance to a class of non-nucleoside inhibitors of the hepatitis C virus NS5B polymerase. *J Biol Chem* 280, 39260-7 (2005)
40. M. P. Walker, & Z. Hong: HCV RNA-dependent RNA polymerase as a target for antiviral development. *Curr Opin Pharmacol* 2, 534-40 (2002)
41. K. Babaoglu, M. A. Page, V. C. Jones, M. R. McNeil, C. Dong, J. H. Naismith, & R. E. Lee: Novel inhibitors of an emerging target in Mycobacterium tuberculosis; substituted thiazolidinones as inhibitors of dTDP-rhamnose synthesis. *Bioorg Med Chem Lett* 13, 3227-30 (2003)
42. S. G. Kucukguzel, A. Kocatepe, E. De Clercq, F. Sahin, & M. Gulluce: Synthesis and biological activity of 4-thiazolidinones, thiosemicarbazides derived from diflunisal hydrazide. *Eur J Med Chem* 41, 353-9 (2006)
43. R. Ottana, S. Carotti, R. Maccari, I. Landini, G. Chiricosta, B. Caciagli, M. G. Vigorita, & E. Mini: *In vitro* antiproliferative activity against human colon cancer cell lines of representative 4-thiazolidinones. Part I. *Bioorg Med Chem Lett* 15, 3930-3 (2005)
44. A. Kumar, C. S. Rajput, & S. K. Bhati: Synthesis of 3-[4'-(p-chlorophenyl)-thiazol-2'-yl]-2-[(substituted azetidinone/thiazolidinone)-aminomethyl]-6-bromoquinazolin-4-ones as anti-inflammatory agent. *Bioorg Med Chem* 15, 3089-96 (2007)
45. M. L. Barreca, A. Chimirri, E. De Clercq, L. De Luca, A. M. Monforte, P. Monforte, A. Rao, & M. Zappala, M. Anti-HIV agents: design and discovery of new potent RT inhibitors. *Farmaco* 58, 259-63 (2003)
46. A. Rao, A. Carbone, A. Chimirri, E. De Clercq, A. M. Monforte, P. Monforte, C. Pannecouque, & M. Zappala: Synthesis and anti-HIV activity of 2,3-diaryl-1,3-thiazolidin-4-ones. *Farmaco* 58, 115-20 (2003)
47. R. K. Rawal, R. Tripathi,S.B. Katti, C. Pannecouque, & E. De Clercq: Design, synthesis, and evaluation of 2-aryl-3-heteroaryl-1,3-thiazolidin-4-ones as anti-HIV agents. *Bioorg Med Chem* 15, 1725-31 (2007)
48. S. G. Kucukguzel, E. E. Oruc, S. Rollas, F. Sahin, & A. Ozbek: Synthesis, characterisation and biological activity of novel 4-thiazolidinones, 1,3,4-oxadiazoles and some related compounds. *Eur J Med Chem* 37, 197-206 (2002)
49. G. Lee, D. E. Piper, Z. Wang, J. Anzola, J. Powers, N. Walker, & Y. Li: Novel inhibitors of hepatitis C virus RNA-dependent RNA polymerases. *J Mol Biol* 357, 1051-7 (2006)
50. N. V. Vo, J. W. Oh, & M. M. Lai: Identification of RNA ligands that bind hepatitis C virus polymerase selectively and inhibit its RNA synthesis from the natural viral RNA templates. *Virology* 307, 301-16 (2003)
51. N. Kaushik, V. N. Pandey, & M. J. Modak: Significance of the O-helix residues of Escherichia coli DNA polymerase I in DNA synthesis: dynamics of the dNTP binding pocket. *Biochemistry* 35, 7256-66 (1996)
52. A. Cornish-Bowden: A simple graphical method for determining the inhibition constants of mixed, uncompetitive and non-competitive inhibitors. *Biochem J* 137, 143-4 (1974)
53. M. Wang, K. K. Ng, M. M. Cherney, L. Chan, C. G. Yannopoulos, J. Bedard, , N. Morin, N. Nguyen-Ba, M. H. Alaoui-Ismaili, R. C. Bethell, & M. N. James: Non-nucleoside analogue inhibitors bind to an allosteric site on HCV NS5B polymerase. Crystal structures and mechanism of inhibition. *J Biol Chem* 278, 9489-95 (2003)
54. W. L. Jorgensen, D. S. Maxwell, & J. Tirado-Rives: Development and testing of the OPLS all-atom force field on conformational energetics and properties of organic liquids. *J Am Chem Soc* 118, 11225-36 (1996)
55. I. Bytheway, & S. Cochran: Validation of molecular docking calculations involving FGF-1 and FGF-2. *J Med Chem* 47, 1683-93 (2004)
56. H. Chen, P. D. Lyne, F. Giordanetto, T. Lovell, & J. Li: On evaluating molecular-docking methods for pose prediction and enrichment factors. *J Chem Inf Model* 46, 401-15 (2006)
57. R. A. Friesner, J. L. Banks,R. B. Murphy, T. A. Halgren, J. J. Klicic, D. T. Mainz, M. P. Repasky, E. H. Knoll, M. Shelley, J. K. Perry, D. E. Shaw, P. Francis, & P. S.Shenkin: P. S. Glide: a new approach for rapid, accurate docking and scoring. 1. Method and assessment of docking accuracy. *J Med Chem* 47, 1739-49 (2004)
58. T. A.Halgren, R. B. Murphy, R. A. Friesner, H. S. Beard, L. L. Frye, W. T. Pollard, & J. L. Banks: Glide: a new approach for rapid, accurate docking and scoring. 2.

Enrichment factors in database screening. *J Med Chem* 47, 1750-9 (2004)
59. M. D. Eldridge, C. W.Murray, T. R. Auton, G. V. Paolini, & R. P.Mee: Empirical scoring functions: I. The development of a fast empirical scoring function to estimate the binding affinity of ligands in receptor complexes. *J Comput Aided Mol Des* 11, 425-45 (1997)
60. T. Kashiwagi, K. Hara, M. Kohara, K. Kohara, J. Iwahashi, N. Hamada, H. Yoshino, & T. Toyoda: Kinetic analysis of C-terminally truncated RNA-dependent RNA polymerase of hepatitis C virus. *Biochem Biophys Res Commun* 290, 1188-94 (2002)
61. N. V. Vo, J. R. Tuler, & M. M. Lai: Enzymatic characterization of the full-length and C-terminally truncated hepatitis C virus RNA polymerases: function of the last 21 amino acids of the C terminus in template binding and RNA synthesis. *Biochemistry* 43, 10579-91 (2004)
62. J. E. Tomassini, K. Getty, M. W. Stahlhut, S. Shim, B. Bhat, A. B. Eldrup, T. P. Prakash, S. S. Carroll, O. Flores, M. MacCoss, D. R. McMasters, G. Migliaccio, & D. B. Olsen,: Inhibitory effect of 2'-substituted nucleosides on hepatitis C virus replication correlates with metabolic properties in replicon cells. *Antimicrob Agents Chemother* 49, 2050-8 (2005)
63. S. S. Carroll, J. E. Tomassini, M. Bosserman, K. Getty, M. W. Stahlhut, A. B. Eldrup, B. Bhat, D. Hall, A. L. Simcoe, R. LaFemina, C. A. Rutkowski, B. Wolanski, Z. Yang, G. Migliaccio, R. De Francesco, L. C. Kuo, M. MacCoss, & D. B. Olsen: Inhibition of hepatitis C virus RNA replication by 2'-modified nucleoside analogs. *J Biol Chem* 278, 11979-84 (2003)
64. Y. Liu, W. W. Jiang, J. Pratt, T. Rockway, K. Harris, S. Vasavanonda, R. Tripathi, R. Pithawalla, & W. M. Kati: Mechanistic study of HCV polymerase inhibitors at individual steps of the polymerization reaction. *Biochemistry* 45, 11312-23 (2006)
65. E. Prentice, J. McAuliffe,X. Lu, K. Subbarao, & M. R. Denison: Identification and characterization of severe acute respiratory syndrome coronavirus replicase proteins. *J Virol* 78, 9977-86 (2004)
66. I. Imbert, J. C. Guillemot, J. M. Bourhis, C. Bussetta, B. Coutard,M. P Egloff, F.Ferron, A. E. Gorbalenya, & B. Canard: A second, non-canonical RNA-dependent RNA polymerase in SARS coronavirus. *Embo J* 25, 4933-42 (2006)
67. X. Xu, Y. Liu, S. Weiss, E. Arnold, S. G. Sarafianos,. & J. Ding: Molecular model of SARS coronavirus polymerase: implications for biochemical functions and drug design. *Nucleic Acids Res* 31, 7117-30 (2003)
68. N. Kaushik, D. Harris, N. Rege, M. J. Modak, P. N. Yadav, & V. N. Pandey: Role of glutamine-151 of human immunodeficiency virus type-1 reverse transcriptase in RNA-directed DNA synthesis. *Biochemistry* 36, 14430-8 (1997)
69. S. Louise-May, W.Yang, X. Nie, D. Liu, M.S. Deshpande, A.S. Phadke, M. Huang, M. & A. Agarwal: Discovery of novel dialkyl substituted thiophene inhibitors of HCV by in silico screening of the NS5B RdRp. *Bioorg Med Chem Lett* 17, 3905-9 (2007)

Abbreviations: HCV: hepatitis C virus; NS5B: HCV non-structural protein 5B; RdRp: RNA-dependent RNA polymerase; SAR: structure–activity relationship; PEG-IFN-alpha: pegylated interferon alpha;, Ni-NTA: nickel-nitrilotriacetic acid; DMSO: dimethylsulphoxide; IPTG: isopropyl-beta-D-thiogalactopyranoside; DTT: dithiothreitol; TP: template-primer; NTP: nucleoside triphosphate; TCA: trichloroacetic acid; NI: nucleoside inhibitor; NNI: non-nucleoside inhibitor; COX: cyclooxygenase enzyme; HIV-1 RT: human immunodeficiency virus type 1; SDS-PAGE: sodium dodecyl sulphate-polyacryalamide gel electrophoresis; PDB: protein data base; E: Enzyme

Key Words: HCV, NS5B, Polymerase inhibitor, SARS, 4-Thiazolidinone, Kinetics

Send correspondence to: Dr. Neerja Kaushik-Basu, Department of Biochemistry and Molecular Biology, UMDNJ-NJMS, 185 South Orange Avenue, Newark, NJ 07103, Tel.: 973-972-8653, Fax: 973-972-5594, E-mail: kaushik@umdnj.edu

http://www.bioscience.org/current/vol13.htm